Gripper Contacts for Part Alignment

Tao Zhang, *Student Member, IEEE*, and Ken Goldberg, *Senior Member, IEEE*

Abstract--For many industrial parts, their resting pose differs from the orientation desired for assembly. It is possible in many cases to compensate for this difference using a parallel-jaw gripper with fixed orientation. The idea is to arrange contact points on each gripper jaw so that the part is aligned as it is grasped. We analyze the mechanics of this alignment based on a combination of toppling, jamming, accessibility, and form closure and describe an $O(n^5 + n^2K)$ algorithm for the design of such gripper contacts, where n is number of edges of the grasped part and K is the description size of the set of placements that put the part in form closure.

Index Terms—Robot grasping, jaw design, part toppling, part feeding.

I. Introduction

Industrial parts on a flat worksurface will naturally come to rest in one of several stable orientations [10], but it is often necessary to rotate a part into a different orientation for assembly [7].

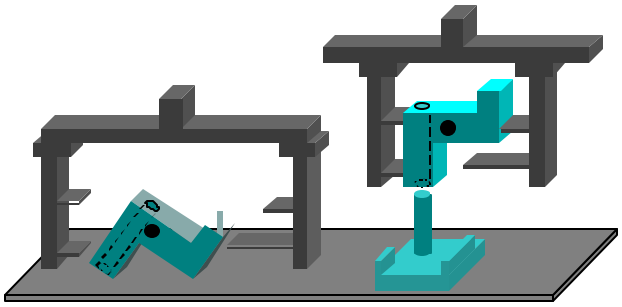

Fig. 1. Gripper jaw contacts align the part for assembly.

This paper proposes an inexpensive (minimalist) method for aligning parts during grasping. As illustrated in Fig. 1, the part is initially in stable orientation (a); it then is rotated by the gripper to orientation (b) for assembly onto the peg.

We achieve this using a simple parallel-jaw gripper with four contacts as shown in Fig. 2. First, toppling contact A and pushing contact A' make contact with the part and topple it from the initial stable orientation to the desired orientation. This phase is referred to as *toppling*. Then, as soon as the part reaches the desired orientation, left fixturing contact B' and right fixturing contact B make contact with the part, stop its rotation, and securely grasp it. This phase is referred to as *grasping*. Note that the pivot point, P, maintains contact with the work-surface at all times.

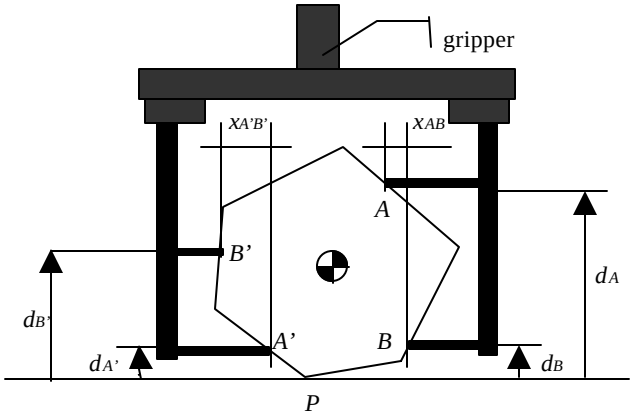

Fig. 2. A and A' topple the part until B and B' combine to produce a form-closure grasp.

These four contacts and the parallel-jaw gripper are designed to be easily reconfigurable to handle different industrial parts, and low in cost, footprint and weight.

II. Related Work

Although grippers has been widely used for automated manufacturing, assembly, and packing, the design of gripper jaws is usually ad-hoc and remains a major limiting factors in robot application. *Proper gripper design can simplify the overall assembly, increase the overall system reliability, as well as decrease the implementation cost* [7].

There is a substantial body of research on robotic grasping; Bicchi and Kumar provide a concise recent survey in [3].

Most work analyses final static grasp configuration. There are a number of 3D theoretical models based on wrench theory. 15 *et al.* [15] prove, by infinitesimal perturbation analysis, that four (seven) hard fingers are necessary and sufficient to achieve form closure of a 2D(3D) object in the absence of friction. Trinkle [25] presents a quantitative test for form-closure grasps in term of linear programming. Ponce *et al.* [18] address the problem of stable grasps of 3D parts and derive necessary and sufficient conditions for equilibrium and force-closure. Rimon and Burdick [20] provide a good summary and extend this work with the notion of 2^{nd} *order immobility*. There is also an extensive body of static analysis of parts in the horizontal plane. Liu [12] presents an $O(n^{3n/2})$ algorithm to compute all n-finger form-closure grasps on a polygonal object. Van der Stappen

T. Zhang is with the Department of Industrial Engineering and Operations Research, and K. Goldberg is with the Department of Industrial Engineering and Operations Research and the Department of Electrical Engineering and Computer Science, University of California, Berkeley, CA 94720-1777 USA.

et al. [22] propose a polynomial-time algorithm to compute all form-closure grasps on a polygonal part with at most four fingers.

A number of papers consider part motion in the horizontal plane and how it can be used to reduce uncertainty. The motion of parts during grasp acquisition is first analyzed by Mason [16], who studies push mechanics as a role of passive compliance in grasping and manipulation. Erdmann and Mason [8] explore the use of motion strategies to reduce uncertainty in the location of objects. They describe a systematic algorithm for sensorless manipulation to orient parts using a tilting tray. Brost [5] applies Mason's Rule to analyze the mechanics of the parallel-jaw gripper and polygonal parts. He shows that it is possible to align parts using passive pushes and squeeze mechanics. Goldberg [9] demonstrates that a modified parallel-jaw gripper can orient polygons up to symmetry by a sequence of normal pushes. Akella *et al*. [2] study a minimalist manipulation method to feed planar parts using a one-joint robot over a conveyor belt.

Several authors address motion of parts in the vertical (gravitational) plane during grasping. Trinkle *et al*. [23][24] show how to align parts in the gravitational plane by lifting them off work-surface using a planar gripper with two pivoting jaws. The pre-liftoff phase analysis of their paper is related to our toppling analysis. They generate *liftability regions* corresponding to possible contacts for the forth finger where causes the object to: slide, jam, break either of two contacts with the surface, or break both contacts with the surface. One important difference is that we focus on how jaw contacts can be designed to align parts using only translational motion. Abell and Erdmann [1] study how a planar polygon can be rotated while stably supported by two frictionless contacts. Zumel and Erdmann [32][33] analyze nonprehensile manipulation using two palms jointed at a central hinge. Erdmann [9] also describes the nonprehensile manipulation in term of C-space, and developed a graph-searching algorithm for a sensorless approach of part orienting. Rao *et al*.[19] give a planar analysis for picking up polyhedral parts using 2 hard-point contacts with a pivoting bearing, allowing the part to pivot under gravity to rotate into a new configuration. Blind *et al*. [4] present a "*Pachinko*"-like device to orient polygonal parts in the vertical plane. It consists of a grid of retractable pins that are programmed to bring the part to a desired orientation as the part falls through.

Causey and Quinn [7] propose guidelines for the design of grippers in manufacturing including: grasp parts securely; include functionality in gripper fingers (jaws); fingers (jaws) should align grasped parts; design for proper gripper-part interaction. This paper provides a new algorithm to address these criteria.

Wallack and Canny [26] develop an algorithm for planning planar grasp configurations using a modular vise. Brown and Brost [6] turn the vise upside down and invent a modular parallel-jaw gripper. Each jaw consists of a regular grid of precisely positioned holes. By properly locating (inserting) four pins on each grid, the object can be grasped reliably at the desired orientation. They give an efficient algorithm for computing optimal positions for pins depending on a planar fixture model and additional 3-D geometry analysis. Kaneko *et al*. [11] derive a sufficient condition for grasping and manipulating parts with multiple contacts. Song *et al*. [21] provide general framework to dynamically simulate multiple contact manipulation.

Our work is also motivated by recent research in toppling manipulation. Zhang and Gupta [28] study how parts can be reoriented as they fall down a series of steps. The authors derive the condition for toppling over a step and defined the transition height, which is the minimum step height to topple a part from a given stable orientation to another. Yu *et al*. [27] estimate the mass and the COM of objects by toppling. Lynch [13] [14] derives sufficient mechanical conditions for toppling parts on a conveyor belt in term of constraints on contact friction, location, and motion. In [29], we describe the *toppling graph* to represent the mechanics and the geometry of toppling manipulation. In this paper, we combine toppling mechanics with an analysis of jamming, accessibility and form-closure in the gravitational plane. A preliminary report on this work appeared in [31].

III. Problem Definition

Given 2D projection of an n-sided convex polyhedral part, how can we rotate the part to a desired orientation and grasp it securely?

The inputs of the problem are: the part's center of mass (COM), vertex clearance radius r, the upper bound of part-surface friction coefficient μ_{s_max}, and the upper bound and the lower bound of part-gripper friction coefficient μ_{t_max} and μ_{t_min}, respectively.

The output of the algorithm is the height of each of the four contacts, d_A, $d_{A'}$, d_B, and $d_{B'}$, as well as the relative x offset between contacts on each jaw, x_{AB}, $x_{A'B'}$ (see Fig. 2). This set of variables determines the gripper contacts that will rotate the part to the desired orientation.

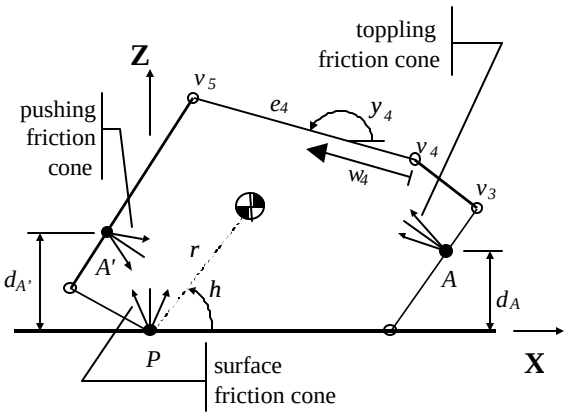

Fig. 3. Notation.

During toppling, only A and A' make contact with the part, and rotate it counterclockwise without causing P to lose contact with the surface. Fig. 3 shows the notation used in the toppling analysis. The part sits on a flat work-surface at a stable orientation. We define a frame originating at P

with X-axis on the surface pointing right and Z-axis pointing up. The frame is not stationery, but moves with P.

Consider the part at its initial orientation, the COM is a distance r from P and an angle h from the +X direction. Starting from the pivot, we consider each edge of the part in counter-clockwise order, namely $e_1, e_2, \ldots, e_n$. The edge e_i, with vertices v_i at (x_i, z_i) and v_{i+1} at (x_{i+1}, z_{i+1}), is in direction γ_i from the +X axis. Let w_i be the distance along edge e_i as shown in Fig. 3. Any point on e_i can be expressed as $(x_i + w_i \cos\gamma_i, z_i + w_i \sin\gamma_i)$.

Let q denote the rotation angle of the part from the +X direction. Initially $q = 0$; $q = q_d$ at the desired orientation. We say an edge e_k is *visible* if it can be seen from +X direction; *invisible*, otherwise. Therefore, e_k is *visible* if $0 < \gamma_k + q < \pi$; e_k is *invisible* if $\pi < \gamma_k + q < 2\pi$. Notice that A can only make contact with visible edges and A' with invisible edges.

We assume that the part and the gripper are rigid, and also that the part's geometry, the location of the COM, and the position of the jaws are known exactly. We also assume that A and A' make contact with the part simultaneously, the part keeps contact with the surface, and the motion of the part and is slow enough that we can ignore inertial effects.

IV. Toppling Analysis

We divide the toppling phase into two sub-phases: rolling and settling, where the COM is to the right/left of A', respectively.

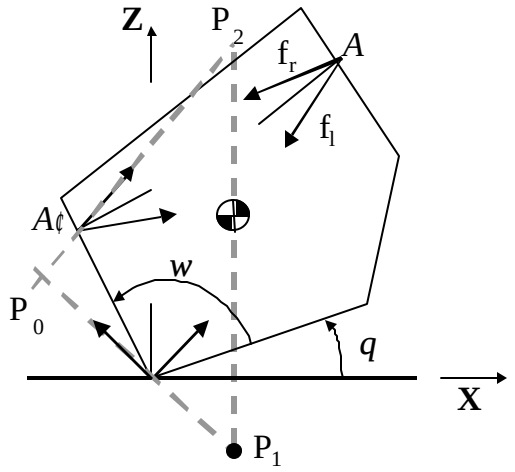

Fig. 4. Rolling conditions ($\pi > w + q > \pi/2$).

As shown in Fig. 4, we assume that A' makes contact with the invisible edge next to P during the entire part alignment process. Similar technique may be applied to other situations (see [30] for details).

Let w denotes the interior angle of the part at P, and let q_t denote the critical rotation angle where the COM is right above A'; therefore,

$$d_{A'} \tan(q_t + w) = r \cos(h + q_t). \quad (1)$$

Our analysis involves the graphical construction of a set of *shape functions* that represent the mechanics of this alignment. All of these functions are dependant on q and map from part orientation to height: $S^1 \rightarrow \hat{\mathbf{A}}^+$, where S^1 is the set of planar orientations.

The *toppling graph* is a combination of some shape functions including the radius function, the vertex function, the rolling function, and the jamming function. In this paper we consider only the range of angles corresponding to rotation from one stable orientation ($q = 0$) to the next ($q = q_n$).

The radius function, $R(q)$, is the height of the COM as the part is rotated. The local minima of the radius function indicate the stable orientations of the part. The vertex function, $V_i(q)$, gives the height of vertex i as the part rotates. Each vertex of the part has a vertex function. Using the vertex functions we can determine which edge the contact makes contact with. Given $d_{A'}$, the range of friction coefficients, and A in contact with edge e_i, the rolling function, $H_i(q)$, is the minimum height of A guarantee to roll the part instantaneously. $H_i(q)$ is determined on the range $q = 0 \sim q_t$. Given $d_{A'}$, the range of friction coefficients, and A in contact with edge e_i, the jamming function, $J_i(q)$, is the minimum height of A to guarantee no jamming.

The combination of these functions forms the toppling graph. Given $d_{A'}$, we can identify d_A that guarantees to topple the part using toppling graph.

First, we consider part-surface and part-gripper friction coefficients are single valued m_s and m_t, respectively. The surface friction cone half-angle is $a_s = \tan^{-1} m_s$, and the pushing/toppling friction cone half-angle is $a_t = \tan^{-1} m_t$. Then, we find $H_i(q)$ and $J_i(q)$ over the given range of m_s and m_t.

A. Rolling Function

During rolling, the part rotates about P, P slides to the right, and the part slips relative to the contacts. The system of forces on the part: the contact force at the surface, the contact force at the contacts, and the part's weight, must generate a positive moment on the part with respect to P. The contact force at P is along the left edge of the surface friction cone. But the direction of the contact force at A' depends on angle $(w + q)$.

Consider the case where $\pi > w + q > \pi/2$. Rotation causes the contact between the part and A' to move away from P. Thus the contact force at A' is along the left edge of the pushing friction cone.

Following the graphical method of Mason [17], we begin by constructing a triangle $P_0P_1P_2$ as shown in Fig. 4. P_0 is at (x_{p0}, z_{p0}), which is the intersection of the left edge of the surface friction cone and the left edge of the pushing friction cone. P_1 is at (x_{p1}, z_{p1}), which is the intersection of the vertical line through the COM and the left edge of the surface friction cone. P_2 is at (x_{p2}, z_{p2}), which is the intersection of the vertical line through the COM and the left edge of the pushing friction cone. Thus, we have:

$$x_{p0} = t - \overline{P_0P_1} \sin a_s, \quad (2)$$

$$z_{p0} = -t/m_s + \overline{P_0P_1} \cos a_s, \quad (3)$$

$$x_{p1} = t, \quad (4)$$

$$z_{p1} = -t/m_s, \quad (5)$$

$$x_{p2} = t, \quad (6)$$

$$z_{p2} = \frac{\frac{d_{A'}}{\tan\varphi} - t}{\tan(\varphi + \alpha_t)}, \quad (7)$$

where $t = r\cos(\theta+\eta)$, $\varphi = w+\eta$ and (8)

$$\overline{P_0P_1} = \frac{(z_{p2} + \frac{t}{m_s})\sin(\varphi + \alpha_t)}{\sin(\varphi + \alpha_t - \alpha_s)}. \quad (9)$$

The locations of P_0, P_1, and P_2 are all the function of η. As η increase, P_1 shrink to P along $\overline{P_0P_1}$, $\overline{P_0P_2}$ sweeps counterclockwise, and P_2 moves up while $\overline{P_1P_2}$ keeps parallel to Z-axis. Triangle $P_0P_1P_2$ exists if and only if $w+\eta+\alpha_t < p$, i.e. $\eta < p-w-\alpha_t$.

Toppling is guaranteed if every force in the toppling friction cone makes a positive moment about every point in the $P_0P_1P_2$ triangle. For all forces in the toppling friction cone to generate a positive moment about the triangle, the left edge of the friction cone must pass above the triangle; all other vectors in the friction cone will pass higher. We denote the vector at the left edge of the toppling friction cone as f_l and the right edge as f_r. We find the height sufficient to roll the edge by projecting lines from P_0, P_1, and P_2 at the angle of f_l until they intersect the edge. The intersection with the maximum height of those three is the minimum height sufficient to roll the part.

Let ${}_2w_i$ denote the toppling contact on edge e_i where f_l passes exactly through point P_2. Let X_i and Z_i denote the location of vertex v_i after conducting pure rotation of η, i.e., $X_i = x_i\cos\eta - z_i\sin\eta$ and $Z_i = x_i\sin\eta + z_i\cos\eta$. We can show through geometric construction that:

$${}_2w_i(\eta) = \frac{Z_i - z_{p2} - (X_i - x_{p2})\tan\gamma_{il}}{\cos\chi_i\tan\gamma_{il} - \sin\chi_i} \quad (10)$$

where $\chi_i = \eta + \gamma_i$ and $\gamma_{il} = \gamma_i + \pi/2 + \alpha_t + \eta$.

Similarly, the toppling contacts for f_l passing through P_0 and P_1 are given by ${}_0w_i(\eta)$ and ${}_1w_i(\eta)$.

The rolling function, $H_i(\eta)$, is based on $w_i(\eta)$ that is max $({}_2w_i(\eta), {}_0w_i(\eta), {}_1w_i(\eta))$ in the rolling region $0 < \eta < \eta_t$. $w_i(\eta)$ can be shown to be:

$$w_i = \begin{cases} {}_2w_i & 0 < \eta < \eta_m \text{ and } \gamma_i < w \\ {}_0w_i & 0 < \eta < \eta_m \text{ and } \gamma_i \geq w \\ \infty & \text{otherwise} \end{cases}, \quad (11)$$

where $\eta_m = \min(\eta_t, p - w - \alpha_t)$. Thus, the rolling function within $0 < \eta < \eta_t$ is given by:

$$H_i(\eta) = \begin{cases} H_i^*(\eta) & V_i(\eta) \leq H_i^*(\eta) \\ 0 & V_i(\eta) > H_i^*(\eta) \end{cases}, \quad (12)$$

where $H_i^*(\eta) = Z_i + w_i\sin\chi_i$. (13)

Following the same methodology, we find $H_i(\eta)$ under the condition $\pi/2 > w+\eta > 0$.

Fig. 5 illustrates function $R(\eta)$, $H_2^*(\eta)$, $V_2(\eta)$ and $V_3(\eta)$ for the part in Fig. 3 with $\alpha_t = 5°$, $\alpha_s = 10°$ and $d_{A'} = 9$mm. The kink ($\eta = 37°$) of $R(\eta)$ represents the orientation where e_6 is on the surface. At a certain angle η, any A at height h will instantaneously rotate the part if $\max(H_2(\eta), V_2(\eta)) < h < V_3(\eta)$. The graph indicates that A can roll the part at any contact on e_2 when $0 < \eta < 20°$.

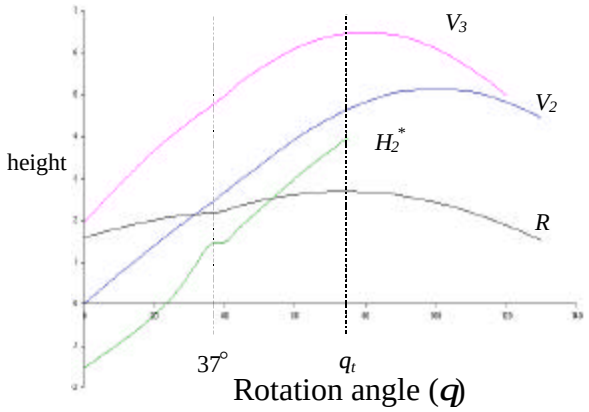

Fig. 5. $R(\eta)$ vs. $H_2^*(\eta)$, $V_2(\eta)$ and $V_3(\eta)$.

B. *Jamming Function*

We allow the part continue to rotate after it reaches η_t if $\eta_d > \eta_t$. We call this process settling and intend to avoid jamming in settling.

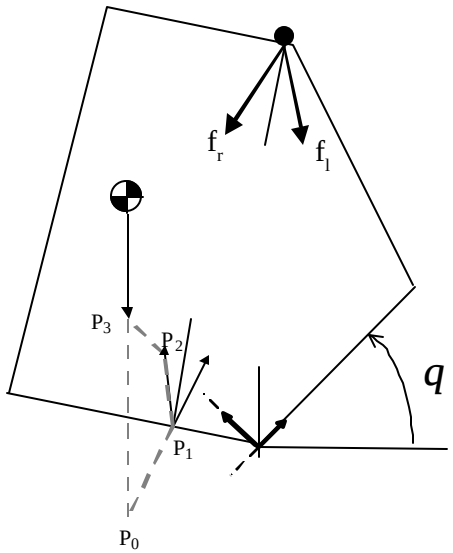

Fig. 6. Jamming conditions.

To determine the jamming function we begin by constructing a primary region as shown in Fig. 6. The primary region is quadrilateral $P_0P_1P_2P_3$. P_0 is at (x_{p0}, z_{p0}), which is the intersection of the vertical line through the part's COM

and the right edge of the pushing friction cone. P_1 is the pushing contact at (x_{p1}, z_{p1}). P_2 is at (x_{p2}, z_{p2}), which is the intersection of the left edge of the pushing friction cone and the left edge of the surface friction cone. P_3 is at (x_{p3}, z_{p3}), which is the intersection of the vertical line through the part's COM and the left edge of the surface friction cone.

Thus, we have:

$$x_{p0} = t, \tag{14}$$

$$z_{p0} = d_{A'} - \frac{d_{A'} \tan \varphi - t}{\tan(\alpha_t - \varphi)}, \tag{15}$$

$$x_{p1} = d_{A'} \tan \varphi, \tag{16}$$

$$z_{p1} = d_{A'}, \tag{17}$$

$$x_{p2} = -\frac{-d_{A'} \cos\alpha_t \sin\alpha_s}{\sin\varphi \sin(\varphi + \alpha_t - \alpha_s)}, \tag{18}$$

$$z_{p2} = \frac{d_{A'} \cos\alpha_t \cos\alpha_s}{\sin\varphi \sin(\varphi + \alpha_t - \alpha_s)}. \tag{19}$$

$$x_{p3} = t, \tag{20}$$

$$z_{p3} = -t/\mu_3. \tag{21}$$

To guarantee that no jamming occurs, any force in the toppling friction cone must not make a negative moment about the primary region; therefore f_1 determines the minimal height at which jamming may occur.

Similar to the analysis of the rolling function, we obtain ${}_2w_i(\theta)$, ${}_0w_i(\theta)$, and ${}_1w_i(\theta)$. When $\theta > \pi - \omega - \alpha_t + \alpha_s$, Quadrilateral $P_0P_1P_2P_3$ doesn't exist and $w_i(\theta)$ is ∞. When $\theta < \pi - \omega - \alpha_t + \alpha_s$, $w_i(\theta)$ is $\min({}_2w_i(\theta), {}_0w_i(\theta), {}_1w_i(\theta))$ and can be shown to be:

$$w_i = \begin{cases} {}_0w_i & \gamma_i < \omega - 2\alpha_t \text{ and } \theta_t < \theta < \theta_{32} \\ {}_1w_i & \omega - 2\alpha_t \le \gamma_i \le \omega \text{ and } \theta < \theta_{32} \\ {}_2w_i & \omega < \gamma_i \text{ and } \theta < \theta_{32} \\ {}_3w_i & \theta_{32} \le \theta \le \theta_d \end{cases} \tag{22}$$

where $\theta_{32} = \pi - \alpha_t - \gamma_i$. (23)

The jamming function, $J_i(\theta)$, with $\theta_t < \theta < \theta_n$ is given by:

$$J_i(\theta) = \begin{cases} J_i^*(\theta) & V_i(\theta) \le J_i^*(\theta) \\ 0 & V_i(\theta) > J_i^*(\theta) \end{cases}. \tag{24}$$

where $J_i^*(\theta) = Z_i + w_i \sin x_i$. (25)

Therefore, for given θ and $d_{A'}$, jamming is guaranteed not to occur if A makes contact with edge e_i and d_A is higher than $J_i(\theta)$.

C. Critical Friction Coefficients

We assume single valued friction coefficients in the last section. Given the range of the friction coefficients, how can we derive the rolling function and the jamming function?

As an example illustrated in Fig. 7, a part is initially at the stable orientation (a) and needed to be rotated 25° to final orientation (b) for assembly. The part is defined by the vertices at (0,0), (51.2, 0), (64.1, 57.2), (37.5, 96.2), (-32.2, 44.6), and COM at (21.9, 42.3). Unit is mm.

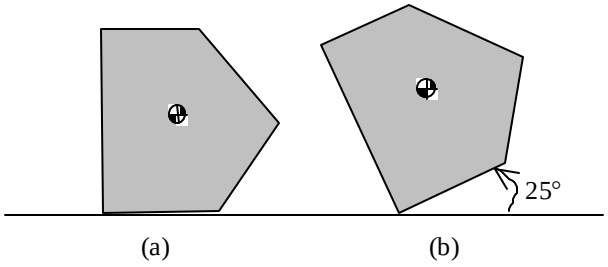

Fig. 7. An example: part alignment.

Therefore, the shape functions are the functions of θ and the friction coefficients. Fig. 8 shows ${}_0w_3$ as the function of α_t and θ given $d_{A'}$ = 5mm and α_s = 10°.

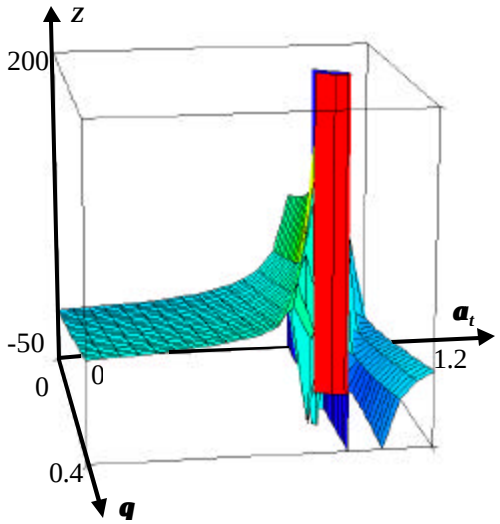

Fig. 8. ${}_0w_i$ as the function of α_t and θ.

We simplify the problem by decomposing the functions into single variable functions. We first consider the functions at each rotation angle θ and derive the conditions for μ_3. Then, given μ_3 and θ, we find the condition for μ_t.

We consider the functions at each θ. For each pair of μ_3 and μ_t in the given range, the rolling function or jamming function is a single value. The maximum of these values is the value of $H_i(\theta)$ or $J_i(\theta)$ at the given θ which corresponds to a certain pair of *critical friction coefficients* in the given range, denoted by μ_3^* and μ_t^*.

We first consider the rolling function. As illustrated in Fig. 4, P_0 moves up along $\overline{P_0P_2}$ as μ_3 decreases. Then, the $P_0P_1P_2$ triangle shrinks, and ${}_0w_i$ decreases while ${}_2w_i$ keeps unchanged. Therefore $H_i(\theta)$ is guaranteed no increment as μ_3 decreases. It is sufficient to consider only the upper bounds of μ_3, i.e. $\mu_3^* = \mu_{3\_max}$, to get $H_i(\theta)$.

Given μ_3^* and θ, the rolling function is a function of μ_t, i.e., $H_i(\mu_t)$. P_2 moves down along $\overline{P_1P_2}$ as μ_t decreases. Therefore, ${}_2w_i$ decreases and $\mu_t^* = \mu_{t\_max}$ for $\gamma_i < \omega$ (where w_i is determined by ${}_2w_i$). But P_0 moves up along $\overline{P_0P_1}$ as μ_t decreases, so we need to determine μ_t^* for $\gamma_i > \omega$ (where w_i

is determined by ${}_0w_i$). We apply numerical search the range of μ_t for maximal w_i, which corresponds to μ_t^* and $H_i(\mu_t)$.

Given $d_{A'}$ = 5mm, μ_s^* = 0.17 and φ =20°, Fig. 9 shows w_3 for the part as a function of α_t. ${}_2w_3$ and ${}_0w_3$ are discontinuous at α_{t_1} = 0.61 and α_{t_2} = 0.78 respectively because of non-existence of primary region $P_0P_1P_2$. As addressed in last section, we only need to consider $H_i(\mu_t)$ when $\alpha_t < \alpha_{t\_1}$, i.e., $\alpha_t < p\text{-}\varphi\text{-}\omega$, where w_3 is determined by ${}_2w_3$.

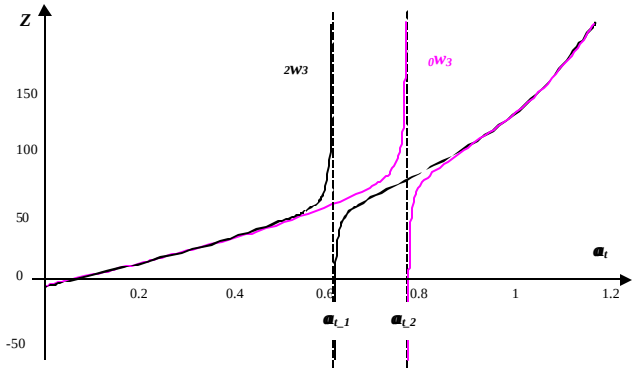

Fig. 9. w_i as the function of α.

We then consider the jamming function given the range of μ_s and μ_t. As illustrated in Fig. 6, P_3 moves up along $\overline{P_0P_3}$ and P_2 moves up along $\overline{P_1P_2}$ as μ_s decreases. Therefore, quadrilateral $P_0P_1P_2P_3$ expands and $J_i(\varphi)$ is guaranteed no increment as μ_s decreases. It is sufficient to consider only the upper bound of μ_s, i.e. $\mu_t^* = \mu_{s\_max}$, to get $J_i(\varphi)$. As μ_t decreases, P_2 moves down along $\overline{P_2P_3}$ and P_0 moves down along $\overline{P_0P_3}$. Therefore, quadrilateral $P_0P_1P_2P_3$ expands and $J_i(\varphi)$ is guaranteed no increment as μ_t decreases. It is sufficient to consider only the upper bound of μ_t, i.e. $\mu_t^* = \mu_{t\_max}$, to get $J_i(\varphi)$.

In summary, we find $H_i(\varphi)$ and $J_i(\varphi)$ over the range of μ_s and μ_t by figuring out the functions at each φ based upon μ_s^* and μ_t^*, where $\mu_s^* = \mu_{s\_max}$ for both functions and $\mu_t^* = \mu_{t\_max}$ for $J_i(\varphi)$. We derive μ_t^* for $H_i(\varphi)$ by numerical method.

D. Toppling Graph

Fig. 10 illustrates the toppling graph that combines the vertex function, the rolling function, and the jamming function for the visible edges. All the rolling functions and the jamming functions correspond to μ_s^* and μ_t^* at each φ. From the toppling graph, d_A can be determined or shown to be non-existent. Note that $H_i(\varphi)$ must be bounded by the $V_i(\varphi)$ and $V_{i+1}(\varphi)$ and is truncated where it intersects them.

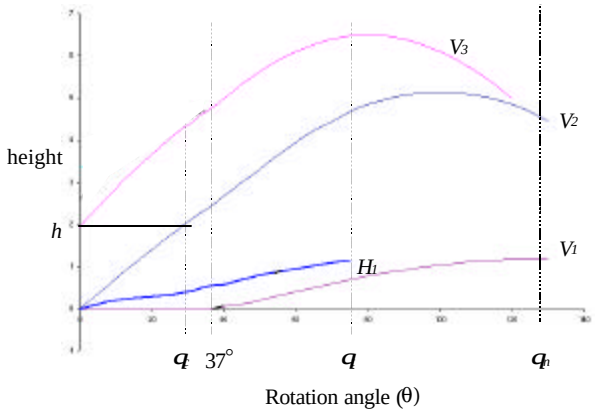

Fig. 10. Toppling graph.

For toppling to be successful there must exist a horizontal line from the angle of the initial orientation to the angle of the desired orientation at height h that has the following characteristics:

1: $h > H_i(\varphi)$, if $V_i(\varphi) < h < V_{i+1}(\varphi)$;
2: $h > J_i(\varphi)$, if $V_i(\varphi) < h < V_{i+1}(\varphi)$;
3: $h < \max_i (V_i(\varphi))$, if $\varphi < \varphi_h$.

where i is the index for the visible edges.

The first two criteria can be described as A must be above both the rolling function and the jamming function of the edge that A makes contact with. When the horizontal line crosses a vertex function, A switches the contact to a new edge and must then be above the rolling function and the jamming function for that edge. The third criterion is that the pin must not lose contact with the part by passing over it during the rolling phase.

Fig. 10 demonstrates the toppling graph of the part shown in Fig. 3. From the graph we can determine the toppling contact at $d_{A'}$ = 2cm is capable to topple the part to any orientation with $0 < \varphi < \varphi_h$. Notice that A switches contact edge from e_2 to e_1 at φ_c.

V. Grasping

Once the part has been rotated to φ_d, the fixturing contacts, B and B', must stop the part rotation and securely grasp it. We additionally require that the combination of the contacts corresponding to A, A', B, and B' generate a form-closure grasp on the part. There also exists an accessibility constraint on the locations of B and B' due to the requirement that they do not block the part's motion trajectory. Therefore, we divide the grasping analysis into two sections on the accessibility and the form-closure requirement, respectively.

A. Accessibility

The accessibility constraint requires that, as the part rotates, it moves out towards the fixturing contacts and at no previous angle has it been touched with the contacts. The accessibility constraint will limit the possible heights of B and B' for given $d_{A'}$ and d_A.

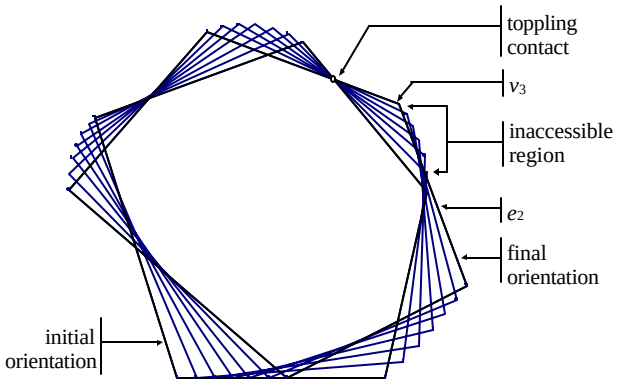

Fig. 11. Rotation of a part relative to the toppling contact A.

In order to determine the accessibility constraint we must consider the relative motion between the part and the gripper. Fig. 11 shows the rotation of a part with respect to A. Note that at any height within the inaccessible range on edge e_2 (at final orientation), vertex v_3 would have contacted B before the part reached the desired orientation.

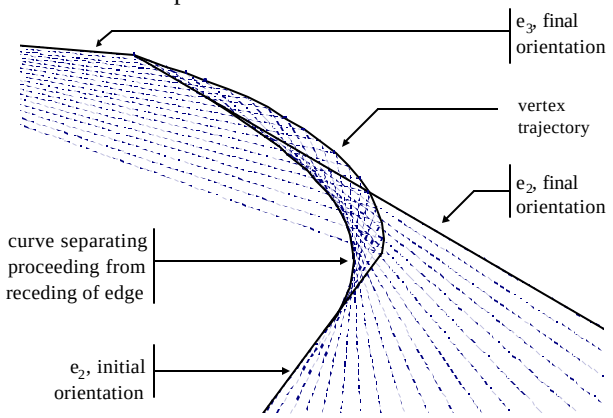

Fig. 12. A portion of the edge in the desired orientation may be blocked in the positive X direction before the part reaches the final orientation. Additionally, a curve shows the separation between where the part is moving forward and where it is receding.

By examining an edge more closely as shown in Fig. 12, all the points below some critical height at θ, denoted h_q, will move out to the part while those above will recede. Therefore, the accessibility constraint requires $d_B \le h_q$ on a given edge at each θ. Let B_q denote a visible point on the part at the height d_B for a given angle θ. Note that B_q is a different physical point for each θ. The relative X distance between A and B_q can be shown geometrically to be:

$$x_q = X_j - X_i + \frac{d_B - Z_j}{\tan \alpha_j} - \frac{d_A - Z_i}{\tan \alpha_i}, \qquad (29)$$

where i and j are the indexes of the edges in contact with A and B respectively. Therefore the derivative of x_q with respect to θ is given by:

$$\frac{dx_q}{d\theta} = Y_i - \frac{d_A - X_i}{\tan \alpha_i} + \frac{d_A - Y_i}{\sin^2 \alpha_j} - Y_j + \frac{d_B - X_j}{\tan \alpha_j} - \frac{d_B - Y_j}{\sin^2 \alpha_j}. \qquad (30)$$

Setting (30) equal to 0 and solving for d_B yields:

$$h_q = d_B = \frac{\left[Y_i - \frac{d_A - X_i}{\tan \alpha_i} + \frac{d_A - Y_i}{\sin^2 \alpha_j} - Y_j - \frac{X_j}{\tan \alpha_j} + \frac{Y_j}{\sin^2 \alpha_j} \right]}{\left[\frac{1}{\tan \alpha_j} - \frac{1}{\sin^2 \alpha_j} \right]}. \qquad (31)$$

For a given edge, only heights less than h_q can be considered to locate B. A similar procedure is used to determine a range of possible $d_{B'}$ for a given $d_{A'}$.

B. *Form-Closure*

At the end of the accessibility considerations we know d_A and $d_{A'}$, as well as ranges of possible values for d_B and $d_{B'}$. From these ranges we must determine d_B and $d_{B'}$ such that the four contacts generate form-closure on the part. Van der Stappen's algorithm [22] gives all placements of point contacts the put a polygonal part in form closure. Therefore, we only need to compare the possible values of d_A, $d_{A'}$, d_B and $d_{B'}$ with the results of Van der Stappen's algorithm. The overlapping areas represent the location of four contacts we look for.

VI. ALGORITHM

We develop a polynomial-time numerical algorithm to solve the problem. An asymptotic upper bound of its running time can be derived as follows.

Given an n-sided polygonal part, there are $O(n)$ invisible edges at the initial orientation of the part. We sample the invisible edges to obtain $d_{A'}$.

For each of $d_{A'}$, we construct the corresponding toppling graph. Since it takes $O(1)$ time to compute each shape function for a visible edge and there are $O(n)$ visible edges in a graph, the running time to obtain a toppling graph is $O(n)$. The toppling graph allows us to identify the feasible range of d_A such that the pair of $(d_A, d_{A'})$ can rotate the part to the desired orientation. Therefore, the total running time it takes to find a pair of feasible $(d_A, d_{A'})$ is $O(n^2)$.

Given a pair of feasible $(d_A, d_{A'})$, we apply $O(n)$ time accessibility analysis to avoid the inaccessible segments for d_B and $d_{B'}$. So it takes time $O(n^3)$ to find a set of four possible contacts, and there are $O(n^2)$ such sets.

Van der Stappen's algorithm runs in $O(n^{2+\varepsilon}+K)$ time for form-closure, where K is the description size of the resulting set of placements and ε is an arbitrarily small constant. For each set of four possible contacts, it takes $O(K)$ time to check its form-closure property.

It is easy to see that this numerical algorithm takes $O(n^{2+\varepsilon}+K) + O(n^2)\ (O(n^3) + O(K)) = O(n^5 + n^2K)$ time. K is bounded by $O(n^4)$, but in most of cases it remains well below the upper bound. We are currently working to identify properties of the graphs that will allow us to give a complete algorithm to compute the optimal jaw shape.

VII. IMPLEMENTATION

We verify our jaw design algorithms by the example in Fig. 7. Fig. 13 illustrates one of many solutions by the algorithm, where A at (5.93, 95.61), A' at (-6.17, 4.55), B at (42.05, 31.83), and B' at (-21.53, 78.02).

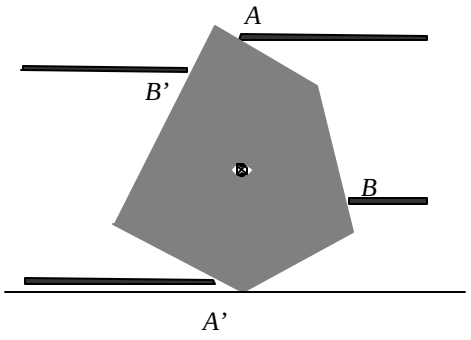

Fig. 13. A resulting jaw design to align the part in gray.

We also conducted a physical experiment using an AdeptOne industrial robot and a parallel-jaw gripper with jaw contacts designed by the methodology described in this paper. The part we used is a small lever from a standard videotape (FUJI serial number: 7410161160). Its planar convex hull is shown in Fig. 3. This part alignment is restricted in the X-Z plane due to the mechanical and the geometric property of the part.

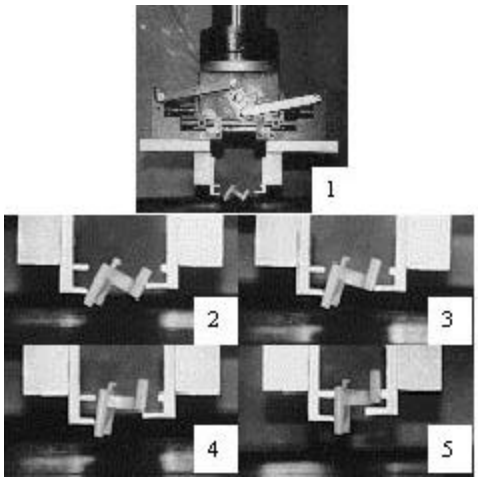

Fig. 14. Part aligning experiment.

Fig. 14 illustrates the successful experiment. The alignment process is showed in sequence 1~5. The part begins at stable orientation in (1). Its desired orientation for insertion is (5) where $\theta = 37°$. We choose A and A' at d_A = 9mm and $d_{A'}$ = 20mm, respectively. The corresponding friction cone half angles are $\alpha_t = 0 \sim 5°$ and $\alpha_s = 0 \sim 10°$. When $\theta < 37°$, P is v_1 and x_2 = 41mm, z_2 = 0mm, $\gamma_2 = 56°$, $\eta = 46°$, ρ = 22mm, and $\omega = 53°$; When $\theta > 37°$, P is v_6 and x_2 = 46mm, z_2 = 24mm, $\gamma_2 = 92°$, $\eta = 55°$, ρ = 27mm, and ω = 89°. The analysis yields the following contact values: d_B = 27mm, $d_{B'}$ = 30mm, x_{AB} = 21mm, and $x_{A'B'}$ = 1mm.

VIII. DISCUSSION AND FUTURE WORK

In industrial practice, gripper jaw geometry is often custom-designed and machined for each part. Design has been ad-hoc and particularly challenging when the part's natural resting pose differs from the desired grip/insertion pose. In this paper we describe a new approach to this problem where 4 contact points on the jaws guide the part into alignment and hold it securely.

The next step is to develop more sophisticated jaw shapes based on part trajectory and to address shape and position uncertainty, friction, and ultimately, 3D geometry. We are also interested in knowing under what conditions a solution exists.

ACKNOWLEDGEMENTS

This paper grew out of practical experiments with a commercial assembly. We would like to thank Brian Carlisle and Randy Brost for suggesting such experiments and Kevin Lynch for his elegant toppling analysis. We would also like to thank RP Berretty and Mark Overmars for their contributions to our thinking about the toppling graph and Gordon Smith for suggesting that toppling could be applied to grasping. Special thanks go to Yong Liu for helpful discussion and K. "Gopal" Gopalakrishnan for careful proofreading. This work was supported in part by the National Science Foundation under CDA-9726389 and Presidential Faculty Fellow Award IRI-9553197. Research funding was also provided by Adept Technology, Ford Motors, and 2000 California State MICRO Grant 00-032.

REFERENCES

[1] T. Abell and M. Erdmann. "Stably supported rotations of a planar polygon with two frictionless Contacts," in *Proc. IEEE/RSJ Int. Conf. Intell. Robots Syst.*, Pittsburgh, 1995, pp. 411-418.

[2] S. Akella, W. Huang, K. Lynch, and M. Mason. "Parts feeding on a conveyor with a one joint robot," *Algorithmica*, Vol.26, No.3-4, pp. 313-344, 2000.

[3] A. Bicchi and V. Kumar. "Robotic grasping and contact: a review. in *Proc. IEEE Int. Conf. Robot. Automat.*, San Francisco, 2000, pp. 348-353.

[4] S. Blind, C. McCullough, S. Akella, and J. Ponce. "A reconfigurable parts feeder with an array of pin," in *IEEE Int. Con. Robot. Automat.*, San Francisco, 2000, pp. 147-153.

[5] R. Brost. "Automatic grasping planning in the presence of uncertainty," *Int. J. Robot. Automat.*, Vol. 7, No. 1, pp. 3-17, 1988.

[6] Brown, R., and R. Brost. "A 3-D modular gripper design tool," *IEEE Trans. Robot. Automat.*, Vol. 15, No. 1, pp. 174-186, 1999.

[7] G. Causey and R. Quinn. "Gripper design guidelines for modular manufacturing," in *IEEE Int. Con. Robot. Automat.*, Leuven, Belgium, 1998, pp. 1453-1458.

[8] M. Erdmann and M. Mason. "An exploration of sensorless manipulation," *IEEE J. Robot. Automat.*, vol. 4, no. 4, 1988, pp. 369-379.

[9] M. Erdmann. "An exploration of nonprehensile two-palm manipulation," *Int. J. Robot. Res.*, vol. 17, no. 5, pp. 485-503, 1998.

[9] K. Goldberg. "Orienting polygonal parts without sensors," *Algorithmica*, vol. 10, no. 2, pp. 201-225, 1993. Special Issue on Computational Robotics.

[10] K. Goldberg, B. Mirtich, Y. Zhuang, J. Craig, B. Carlisle, and J. Canny. "Part pose statistics: estimators and experiments," *IEEE Trans. Robot. Automat.*, vol. 15, no. 5, pp. 849-857, 1999.

[11] M. Kaneko, K. Harada, and T. Tsuji. "A sufficient condition for manipulation of envelop family," in *IEEE Int. Con. Robot. Automat.*, San Francisco, 2000, pp. 1060-1067.

[12] Y. Liu. "Computing *n*-finger form-closure grasps on polygonal objects," *Int. J. Robot. Res.*, vol. 19, no. 2, pp. 149-158, 2000.

[13] K. Lynch. "Toppling manipulation," in *IEEE Int. Con. Robot. Automat.*, Detroit, 1999, pp. 2551-2557.

[14] K. Lynch. "Inexpensive conveyor-based parts feeding," *Assembly Automat.*, vol. 19, no. 3, pp. 209-215, 1999.

[15] X. 15, L. Ni and C. Papadimitriou. "The geometry of grasping," *Int. J. Robot. Res.*, vol. 9, no. 1, pp. 61-74 1990.

[16] M. Mason and J. Salisbury. *Robotic Hands and the Mechanics of Manipulation*, Boston, MA: MIT, 1985.

[17] M. T. Mason. "Two graphical methods for planar contact problems," in *IEEE/RSJ Int. Workshop Intell. Robots Syst.*, Osaka, Japan, 1991, pp. 443-448.

[18] J. Ponce, S. Sullivan, A. Sudsang, J.-D. Boissonnat, and J.-P. Merlet. "On computing four-finger equilibrium and force-closure grasps of polyhedral objects," *Int. J. Robot. Res.*, vol. 16, no. 1, pp. 11-35, 1997.

[19] A. Rao, D. Kriegman and K. Goldberg. "Complete algorithm for feeding polyhedral parts using pivot grasps," *IEEE Trans. Robot. Automat.*, vol. 12, no. 2, pp. 331-342, 1996.

[20] E. Rimon and J. Burdick. "Mobility of bodies in contact-part I: a 2nd-order mobility index for multiple-finger grasps," *IEEE Trans. Robot. Automat.*, vol. 14, no. , pp. 696-708, 1998.

[21] P. Song, M. Yashima, and V. Kumar. "Dynamic simulation for grasping and whole arm manipulation," in *IEEE Int. Con. Robot. Automat.*, San Francisco, 2000, pp. 1082-1087.

[22] A. F. van der Stappen, C. Wentink, and M. Overmars. "Computing immobilizing grasps of polygonal parts," *Int. J. Robot. Res.*, vol. 19, no. 5, pp. 467-479, 2000.

[23] J. Trinkle, J. Abel, R. Paul. "Enveloping frictionless planar grasping," in *IEEE Int. Con. Robot. Automat.*, San Francisco, 1987, pp. 246-251.

[24] J. Trinkle and R. Paul. "Planning for dexterous manipulation with sliding contacts," *Int. J. Robot. Res.*, vol. 9, no. 3, pp. 24-48, 1990.

[25] Trinkle, J. "On the stability and instantaneous velocity of grasped frictionless objects," *IEEE Trans. Robot. Automat.*, vol. 8, no. 5, pp. 560-572, 1992.

[26] A. Wallack and J. Canny. "Planning for modular and hybrid fixtures," *Algorithmica*, vol. 19, no. , pp. 40-60, 1997.

[27] Y. Yu, K. Fukuda and S. Tsujio. "Estimation of mass and center of mass of graspless and shape-unknown object," in *IEEE Int. Con. Robot. Automat.*, Detroit, 1999, pp. 2893-2898.

[28] R. Zhang and K. Gupta. "Automatic orienting of polyhedral through step devices," in *IEEE Int. Con. Robot. Automat.*, Leuven, Belgium, 1998, pp. 550-556.

[29] T. Zhang, G. Smith, R. Berretty, M. Overmars, and K. Goldberg. "The toppling graph: designing pin sequences for part feeding," in *IEEE Int. Con. Robot. Automat.*, San Francisco, 2000, pp. 139-146.

[30] T. Zhang, G. Smith, and K. Goldberg. "Compensatory grasping with the parallel-jaw gripper," Tech. Rep. 00-1, ALPHA lab, UC Berkeley, 2000.

[31] T. Zhang, G. Smith and K. Goldberg. "Compensatory grasping with the parallel-jaw gripper," in *4th Int. Workshop Algorithmic Foundations Robot.*, Hanover, NH, 2000.

[32] N. Zumel and M. Erdmann. "Nonprehensile two palm manipulation with non-equilibrium transitions between stable states," in *IEEE Int. Con. Robot. Automat.*, Minneapolis, 1996, pp. 3317-3323.

[33] N. Zumel and M. Erdmann. "Nonprehensile manipulation for orienting parts in the plane," in *IEEE Int. Con. Robot. Automat.*, Albuquerque, 1997, pp. 2433-2439.